Available online at www.sciencedirect.com

ScienceDirect

IFAC PapersOnline CONFERENCE PAPER ARCHIVE

IFAC PapersOnLine 51-8 (2018) 151–157

Applied Nonlinear Compressor Control with Gain Scheduling and State Estimation

Njål Tengesdal * **Torstein Thode Kristoffersen** ** **Christian Holden** **

* *Corresponding author. Norwegian University of Science and Technology, Norway (e-mail: njaal.tengesdal@ntnu.no).*

** *Norwegian University of Science and Technology, Norway (e-mail: {torstein.t.kristoffersen, christian.holden}@ntnu.no).*

Abstract: Subsea gas compressors are key components for both increased and accelerated hydrocarbon production. Compressors enable the development of fields that are remote, in deep waters, or have low and/or reduced reservoir pressure. In this paper, we present a gain scheduling controller for a nonlinear centrifugal compressor model, coupled with an extended Kalman filter estimating an unmeasured system state. The controller is designed for the normal operating region of a GT2252 turbocharger compressor section, planned for future small-scale experiments. The controller is developed with pole placement design on the equivalent linearized dynamics of the nonlinear model in a set of operating points. The linearized closed-loop system in each operating point is then provably locally asymptotically stable. The controller and estimator are analyzed in simulations, and show to achieve tracking of the desired plenum pressure using the estimate of the compressor mass flow.

Keywords: Compressors, Automation, Nonlinear control, Kalman filters, Feedback control

1. INTRODUCTION

Efficient control of subsea gas compressors enables prolonged production and reduced operational expenses in natural gas fields. A subsea gas compressor is installed upstream of a production facility, typically at the well head, enabling the use of remote satellite wells and production in deeper waters due to an increased differential pressure between the topside equipment and the reservoir. The result is longer plateau production and increased cumulative gas production (Baggerud et al., 2007). A centrifugal compressor is commonly applied due to a versatile operation envelope and robustness to changing flows (Boyce, 1993).

A centrifugal compressor draws the gas flow into its inlet suction port, entering the rotating impeller stage. The impeller increases the kinetic energy of the gas, accelerating the flow. The gas flow exits the impeller stage and is slowed down in the subsequent diffuser stage. In this stage, the kinetic energy is converted to potential energy and thus higher pressure is achieved before the gas is discharged. A detailed derivation of compressor dynamics is given in Egeland and Gravdahl (2002, Ch. 13).

Compressor dynamics are highly nonlinear. A compressor map (Fig. 1) describes the performance and shows the ideal compression process for a specific compressor. The compressor impeller efficiencies are shown in the map as circles around a given constant speed line. The efficiency is a design criteria, and is calculated from the actual work and the thermodynamic process chosen to describe the compression process (Boyce, 1993). The efficiency peaks for the compressor are normally close to the surge line, where the pressure ratio is highest. However, at this line two instabilities (surge and rotating stall) are known to occur when the operating point is shifted to the left of the surge line, i.e., low mass flow and high pressure.

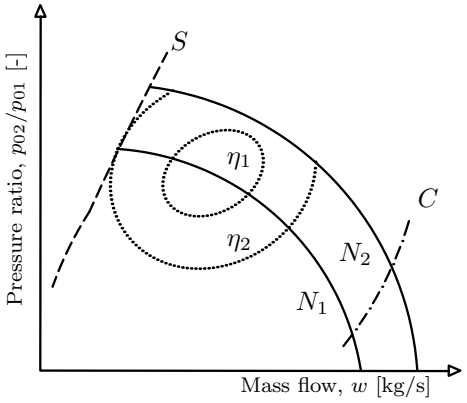

Fig. 1. Compressor map. Efficiency η_i, constant speed lines N_i, choke line C and surge line S.

In academia, several approaches for control design for compressors have been established mainly in terms of active surge control, allowing the compressor to operate in the unstable surge region. In contrast, the more common industrial control method is surge avoidance. In surge avoidance control, surge is avoided by constraining the compressor operational region. Details on active surge control are found in Simon and Valavani (1991), Gravdahl and Egeland (1999) and Shehata et al. (2009) using a

⋆ The research presented in this paper has received funding from the Norwegian Research Council, SFI Offshore Mechatronics, project number 237896.

10.1016/j.ifacol.2018.06.370

close-coupled valve configuration, and Cortinovis et al. (2012) using model predictive control. Compressor control using gain scheduling (GS) has been investigated by, e.g., Tu and Shamma (1998) and Giarré et al. (2006). GS control is either based on a set of linear controllers developed from a set of operating points, or by scheduling the controller gains continuously, derived from a linear parameter varying (LPV) model. A detailed overview of active surge control methods is given in Willems and de Jager (1999), and a survey on GS control is given in Leith and Leithead (2000).

Accurate measurements of pressure and flow are required by most compressor controllers. The measurements are in most cases subject to disturbances from process and measurement noise, which negatively influence the plant controller. The Kalman Filter (KF) is an estimator compensating for system disturbances and estimates unmeasured variables of the system. The KF recursively predicts future system states based on a statistical analysis of the predicted model using inputs and measurements, forming the best estimate from a weighted average of predicted and measured states. The extended Kalman filter (EKF) is a modified KF suitable for nonlinear systems based on linearizing the nonlinear dynamics at the current operating point. The application of EKF stretches from vessel navigation and prediction in meteorology to process control. The EKF is well described in, e.g., Wan and van der Merwe (2000) and Kandepu et al. (2008).

In this paper, we investigate the compressor side of a Garett 2252 turbocharger, which will be used in future small-scale experiments with single and multiphase fluids. A challenge in implementing a controller for the GT2252 setup is that the mass flow is unmeasured at the compressor. The compressor has centrifugal geometry, and is typically used in automobile applications. However, the fundamental operating principles and underlying physics are the same as in a subsea gas compressor facility. Applicability towards a full-scale subsea compressor is therefore assumed to be high.

For the GT2252 setup, surge avoidance is achieved by means of a recycle line controlled by a valve. Therefore, we derive a control system for the normal operating region of the compressor, between the surge line, choke line, and maximum and minimum speed lines in the compressor characteristic. Compressor control is achieved by manipulation of the variable speed drive (VSD) powering the compressor.

We use the GS control method to derive a set of linear controllers, which combined ensures control of the nonlinear plant dynamics. The compressor model used for the control design is the model developed in Gravdahl and Egeland (1999). A state estimator based on the EKF algorithm is developed to estimate the unmeasured mass flow and compensate for disturbances. The performance of the controller and estimator is analyzed in simulations.

The main contribution of this work is the development of a practical control application with combined GS control and estimation of a critical variable for efficient compressor control. To the best of the authors' knowledge, this has not been investigated previously.

The work presented in this paper is an extension of the compressor control design in Tengesdal (2017).

2. COMPRESSOR MODEL

The compression process in a centrifugal compressor is highly nonlinear. The nonlinear axial compressor model developed by Greitzer (1976) is considered state-of-the-art for describing the nonlinear dynamics including surge. Greitzer's model was further proved valid for describing a centrifugal compressor process by Hansen et al. (1981). In Greitzer's work, the static pressure increase is described by a polynomial approximation of the compressor constant speed lines.

A centrifugal compressor model was presented in Gravdahl and Egeland (1999), based on the work by Greitzer (1976). Here, the compression process was modelled as a thermodynamic process (as an isentropic and an isobaric processes in series). Furthermore, the static pressure increase was derived from first principles considering the friction and incidence loss in the impeller originating from the isobaric process. The physical compressor was modelled as three idealized sections where the dynamics of each section is approximated by a lumped parameter model (Fig. 2), representing the distributed model by ordinary differential equations capable of describing surge (Anderson, 1995).

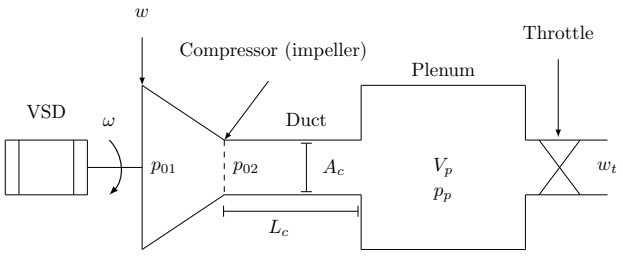

Fig. 2. The centrifugal compressor model.

The ideal compressor component models the static pressure increase, the duct models the mass flow, the plenum models the pressure dynamics and the throttle duct models the discharge mass flow. The duct and plenum form a Helmholtz resonator.

The compressor rotor is mounted on a shaft driven by a VSD supplying the torque. The angular velocity of the shaft is used as the input for the compressor. A detailed derivation of the compressor model is provided in Gravdahl and Egeland (1999).

The two-state compressor model for the compression system in Fig. 2 is given as

$$\dot{p_p} = \frac{a_p^2}{V_p}(w - w_t(p_p) \tag{1}$$

$$\dot{w} = \frac{A_c}{L_c}(\Psi_c(w, \omega)\, p_{01} - p_p) \tag{2}$$

where a_p is the speed of sound of the gas in the plenum, V_p is the plenum volume, w is the compressor mass flow, w_t is the discharge mass flow though the throttle, A_c is the compressor flow-through area, L_c is the effective length of the compressor internal channels, Ψ_c is the pressure ratio characteristic of the compressor, p_{01} is the inlet stagnation pressure and p_p is the plenum pressure. The drive shaft

angular velocity, ω in revolutions per minute (rpm), is considered the control input.

The throttle flow is given by the valve equation for incompressible fluid flow

$$w_t(p_p) = C_d A_t \sqrt{\frac{2}{\rho}(p_p - p_{02})} \tag{3}$$

where C_d is the discharge coefficient, ρ is the gas density, A_t is the throttle valve area and p_{02} is the back pressure from the downstream pipeline.

We consider a simplified approach for deriving the pressure ratio characteristic $\Psi_c(w, \omega)$ approximating the compressor map for the GT2252 turbocharger. The mapped constant speed lines, surge and choke lines and the 78% and 70% efficiency areas are presented in Fig. 3. The control design is focused on the normal operating region of the compressor (between the surge and choke lines). We approximate the characteristic with a 2nd-order polynomial given as

$$\Psi_c(w, \omega) = c_1 + c_2 w + c_3 \omega + c_4 w^2 + c_5 w\omega + c_6 \omega^2 \tag{4}$$

where c_i are constant coefficients.

While Greitzer used a 3rd-order polynomial to describe the pressure ratio characteristic, a 2nd-order polynomial is sufficient in our case as our model only covers the normal operating region. There was negligible difference when fitting a 2nd- or 3rd-order polynomial to the data and so the 2nd-order polynomial was chosen for simplicity. Furthermore, insufficient data from the GT2252 map limited the ability to extend the validity of the model.

The characteristic (4) was fitted to the true characteristic in MATLAB using least squares optimization. The polynomial (4) is shown in Fig. 3 with the optimal characteristic coefficients

$$c = \left[0.737, -1.43, 0.00426, -88.2, 0.145, -1.34 \cdot 10^{-5}\right].$$

However, the polynomial approximation is less accurate for increasing shaft speeds. This will influence the model accuracy when operating the compressor at higher speeds, and the controller will have to compensate for the inaccuracies when used on the real-life compressor.

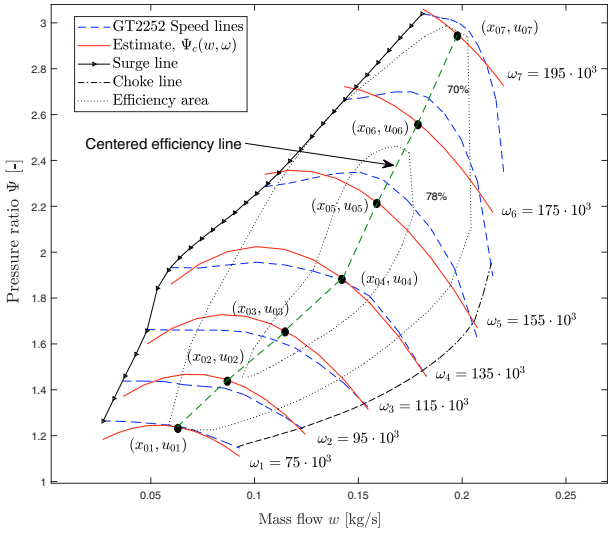

Fig. 3. Estimated characteristic lines for GT2252.

3. GAIN SCHEDULING CONTROLLER

The GS controller presented here is derived from the theory in Khalil (1996, Ch. 12) and Pakmehr et al. (2013). The objective of the GS controller is to achieve offset-free tracking of the plenum pressure reference in the normal operating region of the compressor.

The principle of the GS control method is to switch between linear controller gains depending on the current operating point of the system. Therefore, the GS controller requires a set of linear models for a set of chosen operating points describing the operational envelope.

The compressor map presented in Fig. 3 is defined by 7 constant speed lines, each with a selected operating point $x_{0i}, u_{0i}\ \forall\ i \in \{1, \dots, 7\}$ where $x_{0i} = [x_{0i,1}, x_{0i,2}]^\top$ corresponds to a pressure ratio point and mass flow point, and $u_{0i} = \omega_i$. Each operating point is chosen along the centered efficiency line, intersecting each speed line in the map.

The normal operating region lies between the margins in Fig. 3, i.e., the surge and choke lines. For practical reasons, the origin is shifted to the center of the map creating a new system origin (x_{04}, u_{04}) with minimum distance to each of the operating points. A practical advantage of defining a shifted system origin at (x_{04}, u_{04}) is to have an origin at the point of greatest compressor efficiency. We define the shifted system dynamics in (1) and (2) as

$$\dot{x} = \begin{bmatrix} \gamma k_1 \Big((x_2 + x_{04,2}) - k_t A_t \sqrt{(x_1 + x_{04,1} p_{01} - p_{02}) \frac{1}{\gamma}} \Big) \\ k_2 \left(\Psi_c(x_2 + x_{04,2}, u + u_{04}) \frac{p_{01}}{\gamma} - \frac{(x_1 + x_{04,1} p_{01})}{\gamma} \right) \end{bmatrix} \tag{5}$$

$$y = Cx = [1, 0]x \tag{6}$$

where $k_1 = \frac{a_p^2}{V_p}$, $k_2 = \frac{A_c}{L_c}$, $\dot{x} = f(x, u)$ is the shifted nonlinear model, $x = [p_p - x_{04,1} p_{01}, w - x_{04,2}]^\top$ is the shifted states from the new equilibrium point and u is the step input (rotational speed) from u_{04}. To avoid numerical issues, the plenum pressure is scaled from Pascal to bar using $x_1 = p_p \gamma$, where $\gamma = 10^{-5}$.

To obtain the set of linearized models required by the GS controller, the system dynamics (5) is linearized around each of the operating points. To facilitate for offset-free control of the plenum pressure, (5) and (6) are augmented with an additional integral state $\dot{x}_3 = r - x_1$, where r is the reference pressure. The resulting linearized model is then described by

$$\dot{\tilde{x}} = \begin{bmatrix} A_i & 0 \\ [-1, 0] & 0 \end{bmatrix} \tilde{x} + \begin{bmatrix} B_i \\ 0 \end{bmatrix} u + \begin{bmatrix} \mathbf{0} \\ 1 \end{bmatrix} r \tag{7}$$

$$\tilde{y} = \tilde{C}_i \tilde{x} = [1, 0, 0]\tilde{x} \tag{8}$$

where $\tilde{x} = [x_1, x_2, x_3]^\top$ is the linearized augmented state vector, $A_i = \partial f / \partial x|_{x_{0i}}$ is the Jacobian of the states and $B_i = \partial f / \partial u|_{u_{0i}}$ is the Jacobian of the input.

The GS controller calculates the new control input online by scheduling between the elements in a state feedback gain matrix κ, according to a scheduling variable. In both academia and industry, the scheduling variable is commonly a controlled variable (Khalil, 1996). We develop

our controller by using the plenum pressure reference r as scheduling variable, which determines the desired operating point. The scheduling variable is defined by a limited region $[r_{\min}, r_{\max}]$. If the scheduling variable is selected outside this region (outside the normal operating region of the map), the minimum or maximum value of the state feedback gains in κ is used.

The state feedback gain elements represent the optimal gain at specific operating points. The matrix κ is obtained by offline calculation of the gains for the linearized system (7) and (8) for each of the operating points. The state feedback gains are obtained by pole placement of the eigenvalues in the linearized systems, provided that the system (7) and (8) is controllable. The method is drawn from Chen (1995, Ch. 8). Solving the characteristic equation for each operating point gives a 7 by 3 matrix for κ. The closed-loop linearized system dynamics near the respective operating point is then locally asymptotically stable (Chen, 1995).

To improve robustness and performance, the scheduling part of the GS controller linearly interpolates each element in the state feedback gain matrix κ to form a suitable control input between and at the operating points according to the scheduling variable r. The closest state feedback gain match for the current operating point is given according to

$$\tilde{u} = -\Big(\kappa_{\underline{r}} + (r - \underline{r})\frac{\kappa_{\bar{r}} - \kappa_{\underline{r}}}{\bar{r} - \underline{r}}\Big)\tilde{x} = -K(r)\tilde{x} \tag{9}$$

where $\underline{r}$ is the closest lower operating point, $\bar{r}$ is the closest higher operating point, $\kappa = [\kappa_1, \ldots, \kappa_{i-1}, \kappa_7], \kappa_i = [k_1, k_2, k_3]$ is the resulting gain vector and $\tilde{u}$ is the control input. To constrain the control input to the actuator, the controller is saturated and anti-windup is implemented to avoid the integrator from growing without bounds. The anti-windup procedure is performed via back-calculation of the saturated control input, a method described in Åström and Hägglund (2006). The saturated control input is given as

$$u = \text{sat}(\tilde{u}) = \begin{cases} u_{\max} & \tilde{u} \geq u_{\max} \\ \tilde{u} & u_{\min} < \tilde{u} < u_{\max} \\ u_{\min} & \tilde{u} \leq u_{\min} \end{cases} \tag{10}$$

where $u_{\max}$ and $u_{\min}$ is determined from Fig. 3.

4. ESTIMATOR

An estimator is developed for the compressor system to account for the unmeasured compressor mass flow x_2 that is needed for achieving full state feedback to the GS controller. Provided that the system is observable, an EKF is used to achieve the full state feedback, accounting for the nonlinearities in the system. The EKF can be used for estimation in nonlinear systems using a nonlinear prediction model together with linearized system dynamics to correct for new measurements. The EKF is implemented in discrete time based on Kandepu et al. (2008).

The EKF utilizes a nonlinear discrete-time system model on the form

$$x_{k+1} = f_d(x_k, u_k) + w_k \tag{11}$$
$$y_k = [1,\, 0]x_k + v_k \tag{12}$$

where f_d is obtained by discretizing the nonlinear model (5) and (6) at each sample time with an RK4 method, $w_k \in \mathbb{R}^2$ is the process noise and $v_k \in \mathbb{R}$ is the measurement noise. The noise is modelled as additive white noise $w_k \sim \mathcal{N}(0, Q), v_k \sim \mathcal{N}(0, R)$.

The EKF algorithm uses the nonlinear model to predict the next sample time a priori state estimate $\hat{x}_k^-$ of the system states given the previous sample time aposteriori estimate $\hat{x}_{k-1}$. However, the predicted state error covariance $\hat{P}_k$ is dependent on the linearized, discrete-time system. Therefore, we use exact discretization on the linearised matrices derived in Section 3, updated at every sample time, to calculate the a priori state error covariance $\hat{P}_k^-$. The implemented EKF is summarized in Algorithm 1.

Algorithm 1 Extended Kalman filter

procedure STATE ESTIMATION($\hat{P}_{x_0}$, $\hat{x}_0$)
  while t_{sim} =true **do**
    function ESTIMATOR($\hat{x}_{k-1}$,u_k,$\hat{P}_{k-1}$,Q,R)
      $[\bar{A}_k, \bar{B}_k] = \texttt{discretize}(\frac{\partial f}{\partial \hat{x}_{k-1}}, \frac{\partial f}{\partial u_k}, t_{\text{ds}})$
      $\hat{x}_k^- = f_d(\hat{x}_{k-1}, u_k)$
      $\hat{P}_k^- = \bar{A}_k \hat{P}_{k-1} \bar{A}_k^\top + Q^\top$
      $K_k = \hat{P}_k^- \bar{C}_k^T (\bar{C}_k \hat{P}_k^- \bar{C}_k^\top + R^\top)^{-1}$
      $\hat{x}_k = \hat{x}_k^- + K_k(y_k - \bar{C}_k \hat{x}^-)$
      $\hat{P}_k = (I - K_k \bar{C}_k)\hat{P}_k^- (I - K_k \bar{C}_k)^\top + K_k R K_k^\top$
      return $[\hat{x}, \hat{P}_k]$
    end function
  end while
end procedure

In Algorithm 1, K_k is the optimal Kalman gain, $R = E[vv^T] = \sigma_v^2$ is the measurement covariance matrix and $Q = E[ww^T] = \text{diag}([\sigma_{w_1}^2, \sigma_{w_2}^2])$ is the process covariance matrix. The latter two depend on the knowledge of the system disturbances. These can be determined experimentally, or by tuning. In this paper, we use tuning to obtain values of the covariance for the process and measurement noise.

5. SIMULATION

The performance of the GS controller and estimator performance are analyzed in simulations. Simulation scenarios are based on stepping the compressor though the normal operating region defined by the margins in Fig. 3 while estimating x_2 online using the EKF. The root mean square (RMS) value for both the tracking error $e = r - y$, and the state tracking for the estimator $\hat{e} = x - \hat{x}$ are evaluated. A block diagram of the system is shown in Figure 4.

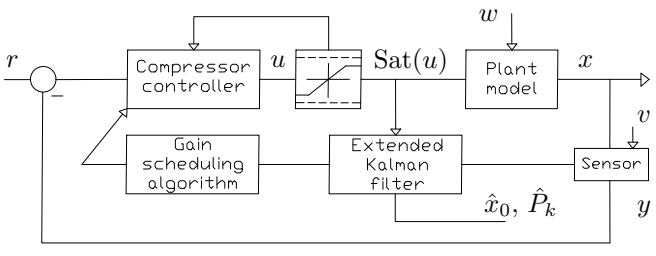

Fig. 4. System block diagram.

Two scenarios are presented in this section. Scenario 1 show the result of simulating the GS controller with constant inlet and back pressures. This scenario is then compared to using a single PI-controller with parameters as in Tengesdal (2017, Chapter 4.5.2). The PI parameters are $K_p = 9.6$ and $T_i = 0.004$ s, tuned with SIMC rules (Skogestad, 2003). The feedback to the PI-controller is the output y, and thus no estimate is needed for the mass flow.

In Scenario 2, time-varying inlet and back pressures are implemented together with GS control. No PI control is used in this scenario. The time-varying inlet and back pressures are modelled as sine functions $p_{0i}(t) = A_{p_{0i}}\sin(\omega_{p_{0i}}t) + p_{0ib}$, where $i \in \{1, 2\}$ (1 is the inlet pressure and 2 is the back pressure). In the simulations, the rpm values were scaled with 10^{-3} for numerical convenience. The parameters for the physical compression system and ambient pressure variables are presented in Table 1.

Table 1. Fixed simulation parameters

L_c [m]	A_c [m^2]	A_t [m^2]	V_p [m^3]	C_d [-]	ρ [$\frac{\text{kg}}{\text{m}^3}$]	p_{01} [bar]	p_{02} [bar]
1.0	0.005	0.0006	0.01	0.6	1.25	1.01325	$1.2p_{01}$

The simulation scenarios where comprised of 8 steps of the pressure reference for the GS controller and estimator. A first-order low-pass filter was included on the reference to smooth the signal, with time constant $T_r = 0.08$ s.

The estimator tuning parameters were set to $R = 0.09$ and $Q = \text{diag}([0.0001, 0.0014])$. The measurement noise variance was set to $\sigma = 0.009$, where the standard deviation is 3 % of an averaged value of 0.3 bar for the measured output. The result after simulating the compressor step response for Scenario 1 is shown in Fig. 5.

As can be seen in Fig. 5, the controller was able to track the desired plenum pressure as the scheduler interpolates between the values in κ upon changes in r. The resulting RMS values for the tracking error and estimator in the first scenario are presented in Table 2.

Table 2. Performance results for the controllers

PI-control law		GS-controller	
RMS$(r-y)$	RMS$(x-\hat{x})$	RMS$(r-y)$	RMS$(x-\hat{x})$
3.7679	[0.0011, $2.70{\cdot}10^{-4}$]	3.7695	[0.0011, $2.73{\cdot}10^{-4}$]

Seen from the result in Table 2 is that the single PI-controller is able to give a marginally lower RMS value for the total simulation run-time. The estimate error for the plenum pressure state is equal in both cases, which is expected since the state was directly measured with measurement signal noise.

The compressor map showing the trajectory for the pressure ratio Ψ_c in each simulation is presented in Fig. 6. During the simulation step scenario the compressor operating point is moved through the new origins.

The difference between the two controllers is best seen in Fig. 6, where the PI-controller moves the operating point past the surge line. Surge did not occur in this simulation; this is due to the model not accurately capturing the dynamics outside the normal operating region, as described in Section 2. Surge should be expected in these conditions if the scenario was repeated on the real compressor.

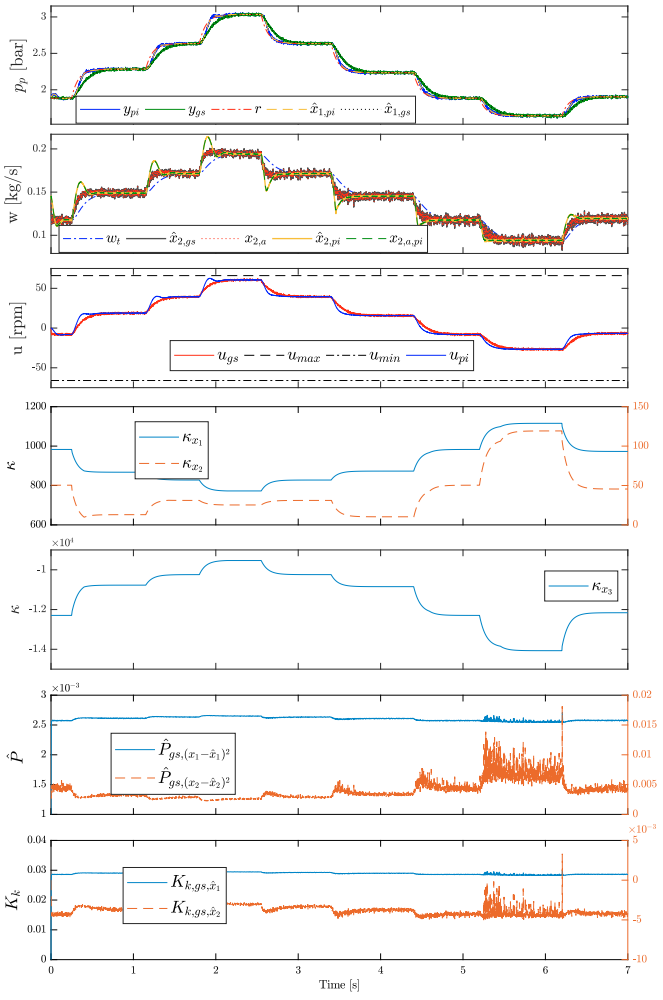

Fig. 5. Simulation result with steps in reference r. The $\hat{x}$ denotes the estimate, and subscripts a, pi and gs are for actual, PI control and GS control respectively.

In the second scenario, the time-varying ambient pressure was used to test the GS controller and estimator robustness. The parameters for the inlet and back pressures are presented in Table 3. The result for scenario two is shown in Fig. 7.

Table 3. Scenario 2 with time-varying pressures

p_{01} [bar]	A_{p1} [bar]	ω_{p01}[rad/s]	p_{02} [bar]	A_{p2} [bar]	ω_{p02}[rad/s]
1.01325	0.01	11	$p_{01} \cdot 1.2$	0.02	8

The varying ambient pressures are seen to influence the mass flow estimate being fed to the GS controller. The ambient pressure amplitudes are relatively low, but causes the mass flow estimate to oscillate. This can be seen by comparing $\hat{x}_2$ in subplot two of Fig. 5 and Fig. 7. The RMS values for Scenario 2 tracking and state error are presented in Table 4.

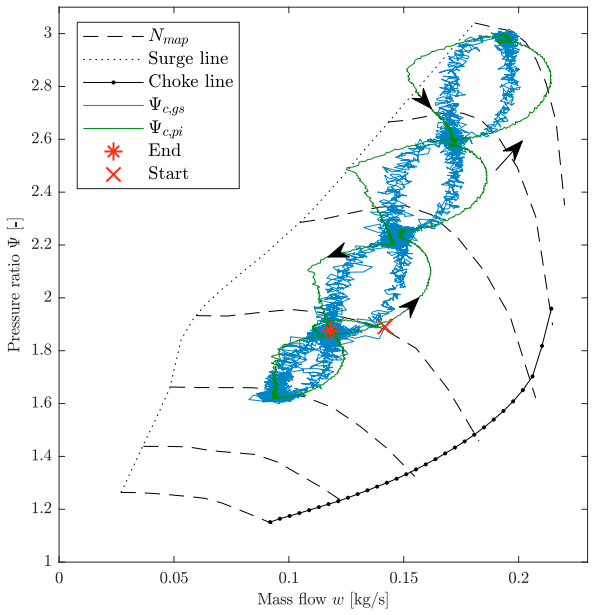

Fig. 6. Compressor map for Scenario 1 with Ψ_c trajectory. The black arrows indicate trajectory direction.

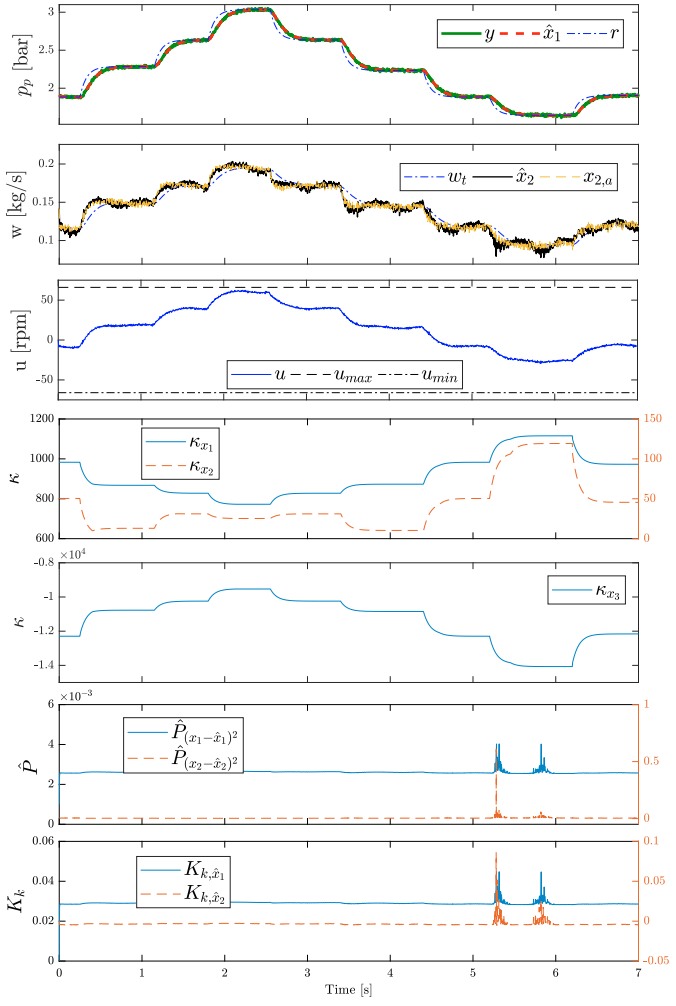

Fig. 7. Scenario 2 with time-varying ambient pressure.

In terms of tracking error the GS controller performs equally as well as it does without varying ambient pressures. However, the state estimation is somewhat poorer (but still of acceptable quality) as can be expected from the more challenging scenario.

Table 4. Scenario 2 performance values

RMS$(r-y)$	RMS$(x-\hat{x})$
3.7695	[0.0017, 0.0034]

The controller and estimator have also been simulated for lower plenum pressure references and mass flow. However, for lower plenum pressures where the mass flow is reduced, the state estimate bias for $\hat{x}_2$ becomes larger (further below operating point x_{03}). Furthermore, this leads to an inaccurate control input, destabilizing the plant model due to poor estimate values fed to the GS controller. As seen in the two lower subplots of both Fig. 5 and Fig. 7 is that for low mass flows (below 0.1 kg/s) $\hat{P}_k$ and K_k experience peaks during step reduction in the simulation. The reason for generating a larger bias is the possibility of poor linearized system dynamics, poorly representing the nonlinear model.

6. CONCLUSION

A gain scheduling controller has been developed for compressor control in the normal operating region, based on a nonlinear compressor model. An EKF algorithm has been used for gas mass flow estimation and disturbance filtering. The scheduling variable is the plenum pressure reference being used by the controller to switch between the designed linear state feedback gains, achieving local asymptotic stability in each operating point.

The GS control algorithm performance has been investigated through simulations and showed to be capable of controlling the compressor to achieve tracking of a desired plenum pressures at varying conditions. The state estimation of the mass flow for operating points in the range x_{03} to x_{07} is achieved and the EKF filter is compensating for the disturbances after proper tuning of the covariance matrices.

6.1 Future work

The simulations provided in this research should be tested and validated in an experimental facility. This should be done to provide enough certainty that the developed GS controller is sufficient for application in real-life scenarios. For extended experiments, the robustness of the controller using the compressor map of a subsea gas compressor being subject to use over time should be investigated.

Due to poor representation of the nonlinear model for lower mass flows further work should include a new estimator for the system capable of eliminating state estimate bias. The analysis may be extended to a full-scale model, with the possibility to implement multi-stage compression.

REFERENCES

Anderson, A. (1995). Simple first-order models for surging in pump and compressor systems. *Proceedings of the Institution of Mechanical Engineers, Part C: Journal of Mechanical Engineering Science*, 209, 149–154.

Åström, K.J. and Hägglund, T. (2006). Advanced PID control. In *The Instrumentation, Systems, and Automation Society*. Citeseer.

Baggerud, E., Halvorsen, V.S., Fantoft, R., et al. (2007). Technical status and development needs for subsea gas compression. In *Offshore Technology Conference*. Offshore Technology Conference.

Boyce, M.P. (1993). Principles of operation and performance estimation of centrifugal compressors. In *Proceedings of Turbomachinery Symposium*, volume 22, 161–177.

Chen, C.T. (1995). *Linear system theory and design*. Oxford University Press, Inc.

Cortinovis, A., Pareschi, D., Mercangoez, M., and Besselmann, T. (2012). Model predictive anti-surge control of centrifugal compressors with variable-speed drives. *IFAC Proceedings Volumes*, 45(8), 251–256.

Egeland, O. and Gravdahl, J.T. (2002). *Modeling and simulation for automatic control*, volume 76. Marine Cybernetics Trondheim, Norway.

Giarré, L., Bauso, D., Falugi, P., and Bamieh, B. (2006). LPV model identification for gain scheduling control: An application to rotating stall and surge control problem. *Control Engineering Practice*, 14(4), 351–361.

Gravdahl, J.T. and Egeland, O. (1999). Centrifugal compressor surge and speed control. *IEEE Transactions on Control Systems Technology*, 7(5), 567–579. doi: 10.1109/87.784420.

Greitzer, E.M. (1976). Surge and rotating stall in axial flow compressors part I: Theoretical compression system model. *Journal of Engineering for Power*, 98, 190.

Hansen, K.E., Jorgensen, P., and Larsen, P.S. (1981). Experimental and theoretical study of surge in a small centrifugal compressor. *Journal of Fluids Engineering, Transactions of the ASME*, 103, 391–395.

Kandepu, R., Foss, B., and Imsland, L. (2008). Applying the unscented Kalman filter for nonlinear state estimation. *Journal of process control*, 18(7), 753–768.

Khalil, H.K. (1996). Noninear systems. *Prentice-Hall, New Jersey*, 2(5), 5–1.

Leith, D.J. and Leithead, W.E. (2000). Survey of gain-scheduling analysis and design. *International journal of control*, 73(11), 1001–1025.

Pakmehr, M., Fitzgerald, N., Feron, E.M., Shamma, J.S., and Behbahani, A. (2013). Gain scheduling control of gas turbine engines: Stability by computing a single quadratic lyapunov function. In *ASME Turbo Expo 2013: Turbine Technical Conference and Exposition*, 1–14. American Society of Mechanical Engineers.

Shehata, R.S., Abdullah, H.A., and Areed, F.F. (2009). Variable structure surge control for constant speed centrifugal compressors. *Control Engineering Practice*, 17(7), 815 – 833.

Simon, J.S. and Valavani, L. (1991). A Lyapunov based nonlinear control scheme for stabilizing a basic compression system using a close-coupled control valve. *Proceedings of the American Control Conference*, 3(4), 2398–2406.

Skogestad, S. (2003). Simple analytic rules for model reduction and PID controller tuning. *Journal of process control*, 13(4), 291–309.

Tengesdal, N. (2017). *Modelling and Control of Dry and Wet Gas Compressors*. Master's thesis, NTNU.

Tu, K.H. and Shamma, J.S. (1998). Nonlinear gain-scheduled control design using set-valued methods. In *American Control Conference, 1998. Proceedings of the 1998*, volume 2, 1195–1199. IEEE.

Wan, E.A. and van der Merwe, R. (2000). The unscented Kalman filter for nonlinear estimation. In *IEEE, Adaptive Systems for Signal Processing, Communications, and Control Symposium 2000*, 153–158.

Willems, F. and de Jager, B. (1999). Modeling and control of compressor flow instabilities. *IEEE control systems*, 19(5), 8–18.